

# Transmission and reflection of a solitary wave in two-dimensional dusty plasma due to an interface

Wei-Ping Zhang<sup>b1</sup> and Wen-Shan Duan<sup>1,†</sup>

<sup>1</sup>College of Physics and Electronic Engineering, Northwest Normal University,  
Lanzhou 730070, PR China

(Received 7 June 2022; revised 5 September 2022; accepted 6 September 2022)

The reflection and transmission of an incident solitary wave with an arbitrary propagation direction due to an interface are investigated in the present paper. It is found that the propagation direction of the transmitted solitary wave depends on not only the propagation direction of the incident solitary wave, but also on the system parameters such as the masses, the number densities of dust particles in two different regions. Dependence of the transmission angle on the plasma parameters and incident angle are given analytically. Moreover, the number and amplitude of transmitted solitary waves and reflected solitary waves are also given when there is only one exact incident solitary wave. Our result has potential application, for example, we can devise an appropriate experiment to measure the differences of the masses and number densities of dust particles between two different regions by using our present results. Furthermore, we can also measure the electric charge of a dust particle by devising an appropriate experiment by using our results.

**Key words:** dusty plasmas, plasma waves, strongly coupled plasmas

---

## 1. Introduction

Dusty plasmas, sometimes called complex plasmas, have been extensively studied during past years (Rao, Shukla & Yu 1990; Mendis & Rosenberg 1994; Barkan, Merlino & D'angelo 1995; Horanyi 1996). Dusty plasmas show many low-frequency phenomena (Duan *et al.* 2004; Ghosh *et al.* 2011; Shukla & Eliasson 2012) due to large mass of dust particles (De Angelis, Formisano & Giordano 1988; Shukla & Silin 1992; Choi, Dharuman & Murillo 2019). Dust acoustic waves (DAW) were first reported theoretically in unmagnetized dusty plasmas by Rao *et al.* (1990). Whereafter, Shukla and Silin found the dust ion acoustic waves (DIAW) (Shukla & Silin 1992). Experiments have confirmed the existence of both DAW and DIAW (Barkan *et al.* 1995; Barkan, D'Angelo & Merlino 1996; Morfill & Thomas 1996). Furthermore, other kinds of waves in a dusty plasma have been reported (D'Angelo & Song 1990; Melzer *et al.* 2000; Wang, Bhattacharjee & Hu 2001; Nunomura *et al.* 2002; Avinash *et al.* 2003; Tsai, Tsai & Lin 2016; Hussain & Hasnain 2017; Marciante & Murillo 2017; Zhang *et al.* 2017; Lin, Murillo & Feng 2020).

† Email address for correspondence: [duanws@nwnu.edu.cn](mailto:duanws@nwnu.edu.cn)

Most of the aforementioned research has focused on a dusty plasma composed of same sized dust particles, however, previous studies have shown that the size of dust particles varies from nanometres to micrometres and their distribution is determined by various conditions. The dust size distribution of dust particles in space plasma can be usually described by a power law distribution (PLD) function (Horanyi & Goertz 1990; Chow, Mendis & Rosenberg 1993; Brattli, Havnes & Melandsø 1997):  $n(r) dr = Kr^{-\beta}$  in the range  $(r_{\min}, r_{\max})$ , while  $n(r) dr = 0$  when  $r < r_{\min}$  or  $r > r_{\max}$ . The dust size distribution of dust particles in laboratory plasma is usually described by a Gaussian distribution (Brattli *et al.* 1997; Meuris, Verheest & Lakhina 1997; Duan 2001):  $n(r) dr = De^{-\mu(r-r_0)^2}$ . Many studies have shown that the dust size distribution can affect the characteristics of a dusty plasma (Duan & Parkes 2003; Duan & Shi 2003; Duan *et al.* 2007).

Recently, a binary dusty plasma containing two types of microparticles of different sizes was studied (Sun *et al.* 2018; Du *et al.* 2019). The binary dusty plasma can either be mixed (Smith *et al.* 2008; Hartmann *et al.* 2009; Wsocki *et al.* 2010; Wieben, Schablinski & Block 2017) or form a phase-separated system (Ivlev *et al.* 2009; Jiang *et al.* 2011; Du *et al.* 2012; Killer *et al.* 2016), caused by spinodal decomposition (Ivlev *et al.* 2009) or an imbalance of external forces (Killer *et al.* 2016). In the latter case, an interface emerges between the separated phases. The propagation of self-excited waves and solitary waves has been investigated in the experiments performed in the PK-3 Plus laboratory on board the International Space Station (ISS) (Yang *et al.* 2017; Sun *et al.* 2018). Furthermore, the reflection and transmission of solitary waves at the low damping regime have been studied by using Langevin dynamics simulations and experiments (Schwabe *et al.* 2008; Menzel, Arp & Piel 2010; Jaiswal *et al.* 2018; Schwabe *et al.* 2020). Later, a theoretical investigation on the propagation of a solitary wave in a phase separated binary complex plasma are given by assuming that the complex plasma is a viscous fluid composed of microparticles (Hong *et al.* 2021). Approximate analytical results of both the transmitted and the reflected waves due to the incident wave whose propagation direction is parallel to the normal direction of the interface are studied analytically, numerically and experimentally (Hong *et al.* 2021). The analytical results are compared with both the simulation results and experimental ones and a qualitative agreement is found. However, only the special case is studied (Hong *et al.* 2021), in which the propagation direction of the incident wave is parallel to the normal one of the interface between two different regions which are composed by two different dust particles. Following this process (Hong *et al.* 2021), the present paper will study the more general case where the propagation direction of the incident wave is arbitrary, i.e. the incident wave angle  $\theta$  (see figure 1) varies in the region  $[0, \pi/2]$ . Dependence of the transmission wave angle  $\alpha$  (see figure 1) on the plasma parameters is shown. Moreover, the number and amplitude of the transmitted solitary waves and the reflected solitary waves are also given.

## 2. Theoretical model

We consider a dusty plasma consisting of dust particles, free electrons and free ions. To study low-frequency phenomena ( $\omega \ll kv_{te}$ ,  $\omega \ll kv_{ti}$ , where  $v_{te}$ ,  $v_{ti}$  are the thermal velocity of electrons and ions), it is customary to treat the electrons and ions as a light fluid which can be modelled by a Boltzmann distribution, while the full set of hydrodynamic equations is used to describe the dynamics of the dust fluid. This is also justified for a strongly coupled regime because of the higher temperatures and smaller electric charges of both electrons and ions (Kaw & Sen 1998). Then, we have  $n_e = n_{e0} \exp(e\phi/k_B T_e)$ ,  $n_i = n_{i0} \exp(-e\phi/k_B T_i)$ , where  $n_e$ ,  $n_i$  are the electron number density and ion number density,

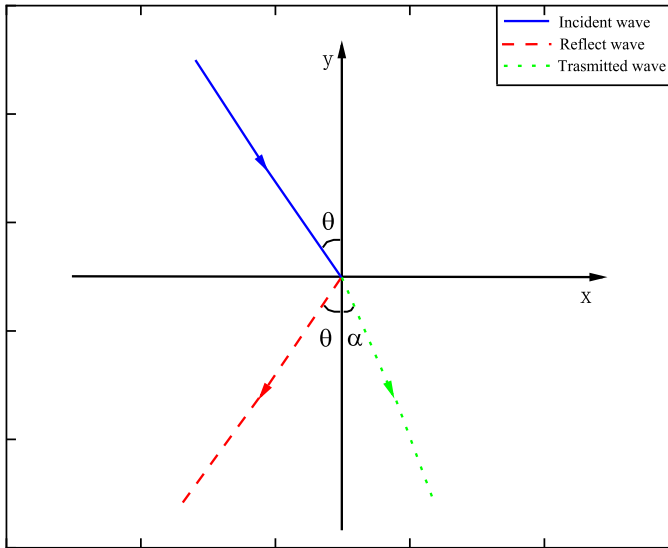


FIGURE 1. Schematic diagram of incident, reflected and transmitted waves. Superscripts ‘*I*’, ‘*R*’ and ‘*T*’ in the text represent incident, reflected and transmitted waves. In the region  $x < 0$ , we use superscript ‘ $-$ ’ to represent all the physical quantities, while in the region  $x > 0$ , we use superscript ‘ $+$ ’ to represent all the physical quantities.

$T_e, T_i$  are the temperatures of electrons and ions,  $\phi$  is electrostatic potential and  $k_B$  is Boltzmann’s constant.

For simplicity and generality, we will study the waves propagating only in the  $xoy$  plane, i.e. the wave number  $\mathbf{k} = (k_x, k_y, 0)$ , for strongly coupled three-dimensional dusty plasma which can be realized not only in the micro-gravity condition but also by using a thermophoretic force as a tool to levitate particles against gravity (Rothermel *et al.* 2002).

We use the generalized hydrodynamic model and introduce a viscoelastic effect and compressibility. The change of dispersion due to the strong coupling effect is mainly caused by compressibility. So, in some cases, the dissipation caused by viscosity and dust collisions is negligible. The neglect of dissipative effects is a valid approximation in the modes with  $\omega\tau_m \gg 1$ , the so-called kinetic modes, where  $\tau_m$  is the relaxation (memory) time. Therefore, the dynamics of the dust fluid in such a strongly coupled dusty plasma is governed by the following normalized equations (Jaiswal, Bandyopadhyay & Sen 2014; Tao *et al.* 2020):

$$\frac{\partial n}{\partial t} + \frac{\partial (nu)}{\partial x} + \frac{\partial (nv)}{\partial y} = 0, \tag{2.1}$$

$$\frac{\partial u}{\partial t} + u \frac{\partial u}{\partial x} + v \frac{\partial u}{\partial y} - \frac{\partial \phi}{\partial x} + \frac{\gamma'}{n} \frac{\partial n}{\partial x} = 0, \tag{2.2}$$

$$\frac{\partial v}{\partial t} + u \frac{\partial v}{\partial x} + v \frac{\partial v}{\partial y} - \frac{\partial \phi}{\partial y} + \frac{\gamma'}{n} \frac{\partial n}{\partial y} = 0, \tag{2.3}$$

$$\frac{\partial^2 \phi}{\partial x^2} + \frac{\partial^2 \phi}{\partial y^2} = n + ve^{\beta s \phi} - \mu e^{-s \phi}, \tag{2.4}$$

where  $n$  refers to the number density of the dust particles,  $u, v$  are the velocities in the  $x$  direction and  $y$  directions,  $s = 1/(\mu + v\beta)$ ,  $C_d^2 = Z_{d0}T_{\text{eff}}/m_d$ ,  $\omega_{pd}^2 = 4\pi n_{d0}Z_{d0}e^2/m_d$ ,

$Z_{d0}$  is the number of charges of a dust particle measured in units of electron charge  $e$  when the dusty plasma is in the equilibrium state,  $\gamma' = \gamma T_d / Z_d T_i$  and  $\gamma$  is the compressibility. We neglect any charge fluctuation of the dust fluid. The compressibility is  $\gamma = (1/T_d)(\partial P_d / \partial n_d) = 1 + u(\Gamma)/3 + (\Gamma/9)(\partial u(\Gamma) / \partial \Gamma)$  (Ichimaru, Iyetomi & Tanaka 1987; Kaw & Sen 1998; Tao *et al.* 2020), where  $\Gamma = Q_d^2 / k_B T_d a$  is the coupling parameter,  $\kappa = a / \lambda_d$  is the screening parameter,  $Q_d = -Z_{d0} e$  is the charge in a dust particle,  $T_d$  is the temperature of the dust fluid,  $d$  is the average distance between dust particles, and  $\lambda_d$  is the Debye length of the dust fluid. Typically, for weakly coupled plasmas  $\Gamma < 1$ ,  $u(\Gamma) = -\frac{\sqrt{3}}{2} u(\Gamma)^{3/2}$  (Kaw & Sen 1998), while in the regime  $1 \leq \Gamma \leq 200$ ,  $u(\Gamma) = -0.89\Gamma + 0.95\Gamma^{1/4} + 0.19\Gamma^{-1/4} - 0.81$  (Kaw & Sen 1998).

### 3. Nonlinear wave

#### 3.1. Poincaré–Lightill–Kuo (PLK) perturbation method

To study the collisions between solitary waves, we adopt the PLK perturbation method and introduce the following coordinate transformations:

$$\xi = \epsilon (x + k_1 y - v_{s1} t) + \epsilon^2 P_0(\eta, \tau) + \epsilon^3 P_1(\xi, \eta, \tau) + \dots, \tag{3.1}$$

$$\eta = \epsilon (x + k_2 y - v_{s2} t) + \epsilon^2 Q_0(\xi, \tau) + \epsilon^3 Q_1(\xi, \eta, \tau) + \dots, \tag{3.2}$$

$$\tau = \epsilon^3 t, \tag{3.3}$$

where  $\epsilon$  is a small parameter,  $\xi$  and  $\eta$  represent the trajectories of two solitary waves,  $v_{s1}$  and  $v_{s2}$  are the velocities of solitary waves propagating in different directions, and  $k_1$  and  $k_2$  are the wave numbers in the  $y$  direction of the first and second solitary waves. Here,  $P_0(\eta, \tau)$  and  $Q_0(\xi, \tau)$  are two quantities which will be determined later, and  $P_1(\xi, \eta, \tau)$  and  $Q_1(\xi, \eta, \tau)$  are another two quantities. We expand the physical quantities as follows:

$$n = 1 + \epsilon^2 n_1(\xi, \eta, \tau) + \epsilon^3 n_2(\xi, \eta, \tau) + \epsilon^4 n_3(\xi, \eta, \tau) + \dots, \tag{3.4}$$

$$u = \epsilon^2 u_1(\xi, \eta, \tau) + \epsilon^3 u_2(\xi, \eta, \tau) + \epsilon^4 u_3(\xi, \eta, \tau) + \dots, \tag{3.5}$$

$$v = \epsilon^2 v_1(\xi, \eta, \tau) + \epsilon^3 v_2(\xi, \eta, \tau) + \epsilon^4 v_3(\xi, \eta, \tau) + \dots, \tag{3.6}$$

$$\phi = \epsilon^2 \phi_1(\xi, \eta, \tau) + \epsilon^3 \phi_2(\xi, \eta, \tau) + \epsilon^4 \phi_3(\xi, \eta, \tau) + \dots. \tag{3.7}$$

#### 3.2. Korteweg de Vries (KdV) equations and their solution

Substituting (3.1)–(3.7) into (2.1)–(2.4), we have the following equations:  $\phi_1 = \phi_\xi(\xi, \tau) + \phi_\eta(\eta, \tau)$ ,  $n_1 = n_\xi(\xi, \tau) + n_\eta(\eta, \tau)$ ,  $u_1 = u_\xi(\xi, \tau) + u_\eta(\eta, \tau)$ ,  $v_1 = v_\xi(\xi, \tau) + v_\eta(\eta, \tau)$ ,  $v_\xi = (k_1 v_{s1} / (\gamma'(1 + k_1^2) - v_{s1}^2)) \phi_\xi$ ,  $u_\xi = (v_{s1} / (\gamma'(1 + k_1^2) - v_{s1}^2)) \phi_\xi$ ,  $n_\xi = ((1 + k_1^2) / (\gamma'(1 + k_1^2) - v_{s1}^2)) \phi_\xi$ ,  $v_\eta = (k_2 v_{s2} / (\gamma'(1 + k_2^2) - v_{s2}^2)) \phi_\eta$ ,  $u_\eta = (v_{s2} / (\gamma'(1 + k_2^2) - v_{s2}^2)) \phi_\eta$ ,  $n_\eta = ((1 + k_2^2) / (\gamma'(1 + k_2^2) - v_{s2}^2)) \phi_\eta$ ,  $n_1 = -s(\nu\beta + \mu)\phi_1$ ,  $v_{s1}^2 = (1 + k_1^2) (\gamma' + 1/Q)$  and  $v_{s2}^2 = (1 + k_2^2) (\gamma' + 1/Q)$ , where  $Q = (\nu\beta + \mu)s$ . The unknown functions  $\phi_\xi(\xi, \tau)$  and  $\phi_\eta(\eta, \tau)$  will be given later. We find from the above equations that there are two waves propagating in two different directions of  $\xi$  and  $\eta$ .

From the higher-order approximation, we have

$$\frac{\partial \phi_\xi}{\partial \tau} + b \phi_\xi \frac{\partial \phi_\xi}{\partial \xi} + c \frac{\partial^3 \phi_\xi}{\partial \xi^3} = 0, \tag{3.8}$$

$$\frac{\partial \phi_\eta}{\partial \tau} + b' \phi_\eta \frac{\partial \phi_\eta}{\partial \eta} + c' \frac{\partial^3 \phi_\eta}{\partial \eta^3} = 0, \tag{3.9}$$

where

$$\left. \begin{aligned} b &= -\frac{1+k_1^2}{2v_{s1}^2Q^2} \left[ v_{s1}(v\beta^2 - \mu)s^2 + \frac{2v_{s1}^3Q^3 + v_{s1}Q^2(1+k_1^2)}{(1+k_1^2)} \right], \\ c &= \frac{1+k_1^2}{2v_{s1}Q^2}, \quad c' = \frac{1+k_2^2}{2v_{s2}Q^2}, \\ b' &= -\frac{1+k_2^2}{2v_{s2}^2Q^2} \left[ v_{s2}(v\beta^2 - \mu)s^2 + \frac{2v_{s2}^3Q^3 + v_{s2}Q^2(1+k_2^2)}{(1+k_2^2)} \right]. \end{aligned} \right\} \quad (3.10)$$

Equations (3.8) and (3.9) are two KdV equations that describe two solitary waves propagating in the  $\xi$  and  $\eta$  directions. The KdV equations have many solutions. One solitary wave solutions of both (3.8) and (3.9) are as follows:

$$\phi_\xi = \frac{3u_{0\xi}}{b} \operatorname{sech}^2 \left[ \left( \frac{u_{0\xi}}{4c} \right)^{1/2} (\xi - u_{0\xi} \tau) \right], \quad (3.11)$$

$$\phi_\eta = \frac{3u_{0\eta}}{b'} \operatorname{sech}^2 \left[ \left( \frac{u_{0\eta}}{4c'} \right)^{1/2} (\eta - u_{0\eta} \tau) \right]. \quad (3.12)$$

The amplitudes and the widths of two solitary waves are  $\phi_{m\xi} = 3u_{0\xi}/b$ ,  $\phi_{m\eta} = 3u_{0\eta}/b'$ ,  $W_\xi = (4c/u_{0\xi})^{1/2}$ ,  $W_\eta = (4c'/u_{0\eta})^{1/2}$ , where  $u_{0\xi}$  and  $u_{0\eta}$  are two arbitrary constants.

### 3.3. The solitary wave solution in the experimental coordinate

To compare our results with the experimental ones, we let all the physical quantities be in the experimental coordinate. Then, one solitary wave solutions of the incident wave, reflected wave and transmitted wave in the experimental coordinate are as follows:

$$u^I = u_m^I \operatorname{sech}^2 \frac{X - V^I t + \epsilon P(\eta, \tau)}{W^I}, \quad (3.13)$$

$$u^R = u_m^R \operatorname{sech}^2 \frac{X' - V^R t + \epsilon Q(\xi, \tau)}{W^R}, \quad (3.14)$$

$$u^T = u_m^T \operatorname{sech}^2 \frac{X - V^T t + \epsilon P(\eta, \tau)}{W^T}, \quad (3.15)$$

where  $u_m^\gamma = u_{m0}^\gamma e^{-(v_d/2)t}$  (Hong *et al.* 2021), where  $\gamma = I, R, T$  which represent incident, reflected and transmitted waves, respectively,  $u_{m0}^\gamma$  is the initial wave amplitude,  $V^\gamma = C_d^\mp + u_m^\gamma/2$  and  $W^\gamma = (1 - u_m^\gamma/2C_d^\mp) \sqrt{4C_d^\mp/u_m^\gamma} \lambda_{Dd}^\mp$ . Notice that the amplitude of the solitary wave decays exponentially due to the viscosity of the dusty plasma. For the low viscosity of a dusty plasma,  $v_d = 0$ , i.e. the amplitude of the solitary wave remains constant. It seems that the propagation speed of the solitary wave increases with the increase of the amplitude of the solitary wave, while the width of the solitary wave decreases with the increase of the amplitude of the solitary wave. Moreover, we have the following equations in the experimental coordinates:  $n^I/n_{d0}^- = u^I/C_d^- = v^I/C_d^- = -\phi^I/(T_{\text{eff}}^-/e)$ ,  $n^R/n_{d0}^- = -u^R/C_d^- = v^R/C_d^- = -\phi^R/(T_{\text{eff}}^-/e)$ ,  $n^T/n_{d0}^+ = u^T/C_d^+ = v^T/C_d^+ = -\phi^T/(T_{\text{eff}}^+/e)$ .

## 4. Inhomogeneity of the dusty plasma

As is well known, most previous studies have assumed that the dust particles in dusty plasma are the same in size, charge and material because it is easier to study. Furthermore,

it is assumed that all dust particles are spherical in shape. However, whether in space plasma or in the laboratory plasma, dust particles of a dusty plasma may differ in size, shape, charge and material composition. Previous studies have shown that the size of dust particles in a space dusty plasma generally satisfies a power law distribution (Horanyi & Goertz 1990; Chow *et al.* 1993; Brattli *et al.* 1997). The size of dust particles of a dusty plasma in experiments generally satisfies a Gaussian distribution (Brattli *et al.* 1997; Meuris *et al.* 1997; Duan 2001). To study the general cases of dust particle size distribution in dusty plasma, some scholars assume that the dust particle size distribution satisfies a polynomial distribution (Chen & Duan 2007; Zhang *et al.* 2016).

#### 4.1. An interface of the dusty plasma

Recently, the propagation of solitary waves in a dusty plasma system composed of different dust particles has been studied theoretically and experimentally. In the experiment, there are two different dusty plasma in two different regions (Sun *et al.* 2018; Du *et al.* 2019; Hong *et al.* 2021). The reflection and transmission of a solitary wave at the interface are studied experimentally and theoretically.

Based on these experiments (Sun *et al.* 2018; Du *et al.* 2019; Hong *et al.* 2021), we now consider a dusty plasma which is made up of two regions. The dusty plasma with smaller dust particles is in the region  $x < 0$ , while the dusty plasma with larger dust particles is in the region  $x > 0$ , see figure 1. Suppose that there is an incident solitary wave in the region  $x < 0$  initially. As it travels to the interface  $x = 0$ , it will be reflected and transmitted at the interface. Therefore, we must consider both reflected and incident waves in the region  $x < 0$ , whereas we only need to consider transmitted waves in the region  $x > 0$ . For simplicity, we use superscripts ‘ $I$ ’, ‘ $R$ ’ and ‘ $T$ ’ to represent incident, reflected and transmitted waves, respectively.

#### 4.2. Evolution of solitary waves from an initial condition

For the sake of convenience, we assume that the incident wave is a single solitary wave and try to know the reflected wave and the transmitted wave. For this reason, we use a previous result (Hong *et al.* 2021). It is well known that the number of solitary waves and their amplitudes can be given from the standard KdV equation and its ‘initial conditions’.

For the standard KdV equation:  $\partial\varphi/\partial t + 6\varphi(\partial\varphi/\partial\xi) + \partial^3\varphi/\partial\xi^3 = 0$  and its ‘initial conditions’:  $\varphi|_{t=0} = -(A/L_0^2)\text{sech}^2(\xi/L_0)$ , where  $L_0$  is the characteristic width of the initial pulse,  $A_0/L_0^2$  is the characteristic amplitude of the initial pulse. The number  $N$  of generated solitary waves and their wave amplitudes for each solitary wave can be given by the following equations:  $\sqrt{A_0 + \frac{1}{4} + \frac{1}{2} - N} > 0$ ,  $2\left(\sqrt{A_0 + \frac{1}{4} + \frac{1}{2} - j}\right)^2 L_0^{-2}$ , where  $j = 1, 2, \dots, N$ . The number  $N$  is the maximum integer.

The three KdV equations for the incident wave, reflected wave and transmitted wave can be rewritten as follows:

$$\frac{\partial\phi_\xi^I}{\partial\tau} + b^-\phi_\xi^I\frac{\partial\phi_\xi^I}{\partial\xi} + c^-\frac{\partial^3\phi_\xi^I}{\partial\xi^3} = 0, \quad (4.1)$$

$$\frac{\partial\phi_\eta^R}{\partial\tau} + (b')-\phi_\eta^R\frac{\partial\phi_\eta^R}{\partial\eta} + (c')-\frac{\partial^3\phi_\eta^R}{\partial\eta^3} = 0, \quad (4.2)$$

$$\frac{\partial\phi_\xi^T}{\partial\tau} + b^+\phi_\xi^T\frac{\partial\phi_\xi^T}{\partial\xi} + c^+\frac{\partial^3\phi_\xi^T}{\partial\xi^3} = 0, \quad (4.3)$$

where superscript ‘-’ represents the values in the region  $x < 0$ , while superscript ‘+’ stands for the values in the region  $x > 0$ , where  $\phi^\gamma = \epsilon^2 \phi_1^\gamma$ ,  $\gamma = I, R, T$ ,  $\phi^\gamma$  represents the electrostatic potential of the wave  $\gamma$  in the experimental coordinate, and the coefficients of the KdV equation are

$$\left. \begin{aligned} b &= -\frac{1+k_1^2}{2v_{s1}^2 Q^2} \left[ v_{s1}(\nu\beta^2 - \mu)s^2 + \frac{2v_{s1}^3 Q^3 + v_{s1} Q^2(1+k_1^2)}{(1+k_1^2)} \right], \\ c &= \frac{1+k_1^2}{2v_{s1} Q^2}, \quad c' = \frac{1+k_2^2}{2v_{s2} Q^2}, \\ b' &= -\frac{1+k_2^2}{2v_{s2}^2 Q^2} \left[ v_{s2}(\nu\beta^2 - \mu)s^2 + \frac{2v_{s2}^3 Q^3 + v_{s2} Q^2(1+k_2^2)}{(1+k_2^2)} \right]. \end{aligned} \right\} \quad (4.4)$$

### 5. Reflection and transmission of incident solitary waves

To know how an incident solitary wave is reflected and transmitted due to an interface, we have to know the quasi-initial conditions of the reflected and transmitted waves from the incident waves by the following continuity conditions at the interface.

#### 5.1. Continuity conditions at the interface

Neglecting higher-order quantities, we give the continuity conditions at the interface  $x = 0$ . The continuous conditions at the interface are electrostatic-potential and momentum:

$$[\phi^I + \phi^R]_{x=0} = \phi^T|_{x=0}, \quad (5.1)$$

$$m_d^- n_{d0}^- [u^I + u^R]_{x=0} = m_d^+ n_{d0}^+ u^T|_{x=0}, \quad (5.2)$$

$$m_d^- n_{d0}^- [v^I + v^R]_{x=0} = m_d^+ n_{d0}^+ v^T|_{x=0}, \quad (5.3)$$

where momentum is a vector; therefore, there are two components of momentum in the  $x$  and  $y$  directions. Equations (5.1), (5.2) and (5.3) are in the experimental coordinate. We have the ‘initial conditions’ of the reflected and the transmitted waves from (5.1), (5.2) and (5.3):

$$\phi^T|_{x=0} = \frac{2}{1+\chi} \phi^I|_{x=0}, \quad (5.4)$$

$$\phi^R|_{x=0} = \frac{1-\chi}{1+\chi} \phi^I|_{x=0}, \quad (5.5)$$

where  $\chi = m_d^+ n_{d0}^+ C_D^+ T_{\text{eff}}^- / m_d^- n_{d0}^- C_D^- T_{\text{eff}}^+$ . We assume that the incident wave is a single solitary wave given by the standard KdV equation and the following initial conditions:

$$\frac{\partial \phi^I}{\partial t} + 6\phi^I \frac{\partial \phi^I}{\partial \xi} + \frac{\partial^3 \phi^I}{\partial \xi^3} = 0, \quad (5.6)$$

$$\phi^{(I)}_{(\xi, \tau)} = -\frac{2}{W^2} \text{sech}^2 \left( \frac{\xi}{W} - \frac{4\tau}{W^2} \right), \quad (5.7)$$

where  $W$  is the wave width. When the incident solitary wave propagates from the region  $x < 0$  to the interface  $x = 0$ , it will be reflected and transmitted. The equivalent

‘initial conditions’ of reflected wave and transmitted wave can be given by the boundary conditions of (5.4) and (5.5):

$$\varphi^{(T)}_{(t_T,0)} = \frac{A_T}{(L_T)^2} \operatorname{sech}^2 \left( \frac{t_T}{L_T}, 0 \right), \tag{5.8}$$

$$\varphi^{(R)}_{(t_R,0)} = \frac{A_R}{(L_R)^2} \operatorname{sech}^2 \left( \frac{t_R}{L_R}, 0 \right), \tag{5.9}$$

where  $A_T = 2A_0(1/(1 + \chi))(T_{\text{eff}}^-/T_{\text{eff}}^+)$ ,  $L_T = L_0$ ,  $A_R = A_0((1 - \chi)/(1 + \chi))$ ,  $L_R = L_0$ ,  $A_0 = 2$ . The ‘initial conditions’ of the reflected and transmitted waves can be used to determine the number of reflected and transmitted solitary waves and the amplitudes of each reflected solitary wave and each transmitted solitary wave generated by the incident solitary wave after a period of evolution.

It seems that the number of reflected and transmitted solitary waves is in agreement in the special case that the propagation direction of the incident wave is parallel to the normal direction of the interface (Hong *et al.* 2021).

### 5.2. Dependence of the transmitted wave angle $\alpha$ on the incident wave angle $\theta$

In this section, we will discuss how the quantity  $\alpha$  depends on the quantity  $\theta$  when the incident wave hits the interface arbitrarily. We assume that the angle of the incident solitary wave is  $\theta$  and the angle of the reflected solitary wave is equal to that of the incident solitary wave. However, the angle of the transmitted solitary wave is usually different from that of the incident solitary wave. Therefore, we assume that the angle of the transmitted solitary wave is  $\alpha$ . Notice from figure 1 that  $v^l = u^l \operatorname{ctg} \theta$ ,  $v^R = -u^R \operatorname{ctg} \theta$  and  $v^T = u^T \operatorname{ctg} \alpha$ . Then we have

$$\frac{\tan \alpha}{\tan \theta} = \chi, \tag{5.10}$$

where  $\chi = m_d^+ n_{d0}^+ C_d^+ T_{\text{eff}}^- / m_d^- n_{d0}^- C_d^- T_{\text{eff}}^+$ , and (5.10) is the relation between  $\theta$  and  $\alpha$ . To know the dependence of  $\alpha$  on  $\theta$ , we use the result (Wang *et al.* 2016):  $Q_d = k_q' \cdot m_d^{2/3}$ , where  $k_q'$  is a constant, and it is estimated that  $k_q' = -3.204 \times 10^{-6}$ . It is easy to be verified as follows. The charge of the dust particles is generally proportional to the square of their radius (Wang *et al.* 2016), while the mass of the dust particles is proportional to the cubic power of their radius.

Notice that the dependence of  $\alpha$  on  $\theta$  is equivalent to the dependence of the parameter  $\chi$  on the parameters of the dusty plasma, such as the number density, the mass, the temperature, the charge of dust particles, as well as the number density, and the temperatures of both electrons and ions.

Figure 2 shows the dependence of  $\chi$  on the mass  $m^+$  and  $m^-$  of dust particles in the region  $x > 0$  and  $x < 0$ , respectively, for the three-dimensional case, where  $n_{d0}^+ = n_{d0}^- = 10 \times 10^9 \text{ m}^{-3}$ ,  $n_{e0} = 1.0 \times 10^{14} \text{ m}^{-3}$ ,  $T_e = 5 \text{ eV}$ ,  $T_i = 0.1 \text{ eV}$  and  $T_d = 298 \text{ K}$  (Du *et al.* 2012). Notice from figure 2 that  $\chi = 1$  when  $m^+ = m^-$ , i.e. if the masses of the dust particles in two different regions are same,  $\alpha = \theta$ . It is noted from figure 2 that  $\alpha$ , or  $\chi$ , increases as the mass of the dust particles in the region  $x > 0$  increases, while it decreases as the mass of the dust particles in the region  $x < 0$  increases.

Figure 3 shows the dependence of  $\chi$  on the number density  $n_{d0}^+$  and  $n_{d0}^-$  of the dust particles in the region  $x > 0$  and  $x < 0$ , respectively, for the three dimensional case, where  $m^+ = m^- = 5.0 \times 10^{-15} \text{ kg}$ ,  $n_{e0} = 1.0 \times 10^{14} \text{ m}^{-3}$ ,  $T_e = 5 \text{ eV}$ ,  $T_i = 0.1 \text{ eV}$  and  $T_d = 298 \text{ K}$  (Du *et al.* 2012). Notice from figure 3 that  $\chi = 1$  when  $n_{d0}^+ = n_{d0}^-$ , i.e. if the number density of dust particles in two different regions are the same,  $\alpha = \theta$ . It is also

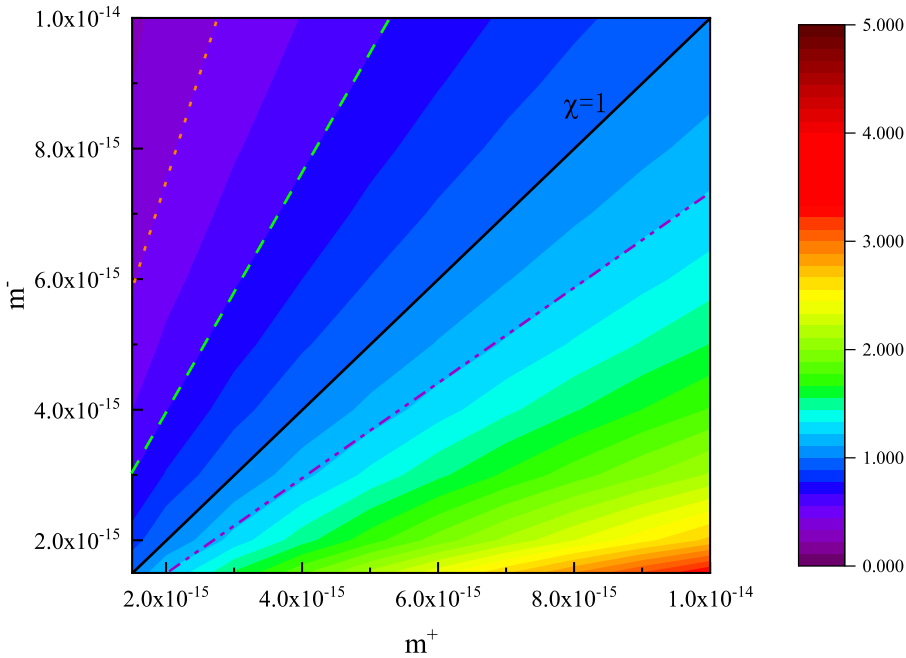


FIGURE 2. In the three-dimensional case, the influence of dust particle mass  $m^+$  and  $m^-$  on parameter  $\chi$ , where the orange line is  $\chi = \frac{1}{4}$ ,  $\tan \alpha = \frac{1}{4} \tan \theta$ , the green line is  $\chi = \frac{1}{2}$ ,  $\tan \alpha = \frac{1}{2} \tan \theta$ , the black line is  $\chi = 1$ ,  $\tan \alpha = \tan \theta$ , the purple line is  $\chi = \frac{3}{2}$ ,  $\tan \alpha = \frac{3}{2} \tan \theta$ , and the other system parameters are  $n_{d0}^+ = n_{d0}^- = 10 \times 10^9 \text{ m}^{-3}$ ,  $n_{e0} = 1.0 \times 10^{14} \text{ m}^{-3}$ ,  $T_e = 5 \text{ eV}$ ,  $T_i = 0.1 \text{ eV}$  and  $T_d = 298 \text{ K}$ .

noted from figure 3 that  $\alpha$ , or  $\chi$ , increases as the number density of the dust particles in the region  $x > 0$  increases, while it decreases as the number density of the dust particles in the region  $x < 0$  increases.

The dependences of  $\chi$  on the ion number density  $n_{e0}$ , the dust particle temperature  $T_d$ , the electron temperature  $T_e$  and the ion temperature  $T_i$  in both regions of  $x > 0$  and  $x < 0$  for the given system parameters have also been studied. It seems that all have no effect on  $\chi$ . Therefore,  $\alpha$  is independent of ion number density, and the temperatures of electrons, ions and dust particles.

The dependence of  $\alpha$  on  $\theta$  has potential applications. For example, though the dependence of the electric charge on the dust size is usually in the form (Wang *et al.* 2016):  $Q_d \propto r_d^p$ , where  $r_d$  is the size of a dust particle,  $1 < p \leq 2$  (Wang *et al.* 2016). The electric charge of a dust particle may be positive in certain conditions. To know the electric charge of a dust particle, we may try to devise an experiment to detect the electric charge of a dust particle by the following process. The parameter  $\chi$  can be rewritten as follows:

$$\chi = \frac{\sqrt{m_d^+ n_{d0}^+} \sqrt{Z_{d0}^+} \sqrt{T_{\text{eff}}^-}}{\sqrt{m_d^- n_{d0}^-} \sqrt{Z_{d0}^-} \sqrt{T_{\text{eff}}^+}}. \tag{5.11}$$

It is easy to give the mass, the number density and the effective temperature of the dust particles in two different regions. After given these parameters, let an incident solitary wave propagate in an incident wave angle  $\theta$ , measure the transmitted wave angle  $\alpha$ , and then we can obtain the ratio of parameter  $Z_{d0}^+$  to  $Z_{d0}^-$ . If one of them is given, then the other

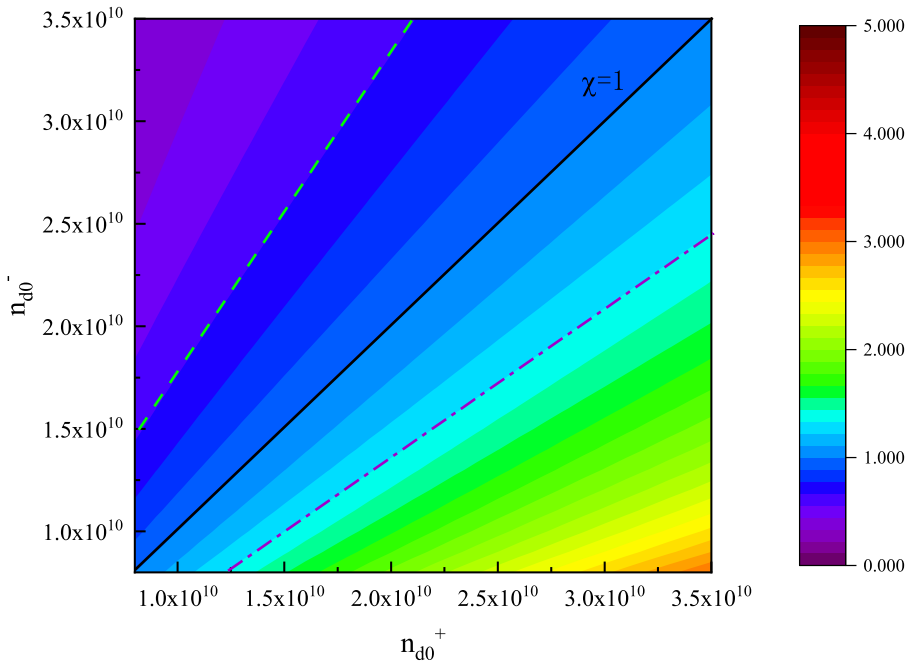


FIGURE 3. In the three-dimensional case, the influence of dust particle number density  $n_{d0}^+$  and  $n_{d0}^-$  on the system parameter  $\chi$ , where the green line is  $\chi = \frac{3}{5}$ ,  $\tan \alpha = \frac{3}{5} \tan \theta$ , the black line is  $\chi = 1$ ,  $\tan \alpha = \tan \theta$ , the purple line is  $\chi = \frac{3}{2}$ ,  $\tan \alpha = \frac{3}{2} \tan \theta$ , and the other system parameters are  $m^+ = m^- = 5.0 \times 10^{-15}$  kg,  $n_{e0} = 1.0 \times 10^{14}$  m $^{-3}$ ,  $T_e = 5$  eV,  $T_i = 0.1$  eV and  $T_d = 298$  K.

is obtained. This result can be used to measure the electric charge of a dust particle in a dusty plasma.

## 6. Conclusion

Based on the magnetohydrodynamical model, we studied the reflection and the transmission of an arbitrary propagation direction incident wave due to an interface between two different regions of a dusty plasma. This investigation is different from the previous results in which the propagation direction of the incident wave is parallel to the normal direction of the interface (Hong *et al.* 2021). It is found that the transmitted wave angle depends on the system parameters such as the masses of the dust particles and the number densities of the dust particles in two different regions. Dependence of the transmitted wave angle on the plasma parameters and the incident wave angle are given. Moreover, the number and the amplitude of the transmitted solitary waves and the reflected solitary waves are also given.

Based on the present investigation results, we can estimate the differences of the dust particles such as the masses and number densities of dust particles between two different regions by devising an appropriate experiment. We can also devise an experiment to measure the electric charge of the dust particles.

## Acknowledgements

This work was supported by the National Natural Science Foundation of China (NSFC) under the grant Nos. 11965019, 42004131 and 42065005.

Editor Edward Thomas, Jr. thanks the referees for their advice in evaluating this article.

### Declaration of interests

The authors report no conflicts of interest.

### REFERENCES

- AVINASH, K., ZHU, P., NOSENKO, V. & GOREE, J. 2003 Nonlinear compressional waves in a two-dimensional yukawa lattice. *Phys. Rev. E* **68** (4), 046402.
- BARKAN, A., D'ANGELO, N. & MERLINO, R.L. 1996 Experiments on ion-acoustic waves in dusty plasmas. *Planet. Space Sci.* **44** (3), 239–242.
- BARKAN, A., MERLINO, R.L. & D'ANGELO, N. 1995 Laboratory observation of the dust-acoustic wave mode. *Phys. Plasmas* **2** (10), 3563–3565.
- BRATTLI, A., HAVNES, O. & MELANDSØ, F. 1997 The effect of a dust-size distribution on dust acoustic waves. *J. Plasma Phys.* **58** (4), 691–704.
- CHEN, J.H. & DUAN, W.S. 2007 Instability of waves in magnetized vortex-like ion distribution dusty plasmas. *Phys. Plasmas* **14** (8), 083702.
- CHOI, Y., DHARUMAN, G. & MURILLO, M.S. 2019 High-frequency response of classical strongly coupled plasmas. *Phys. Rev. E* **100** (1), 013206.
- CHOW, V.W., MENDIS, D.A. & ROSENBERG, M. 1993 Role of grain size and particle velocity distribution in secondary electron emission in space plasmas. *J. Geophys. Res.* **98** (A11), 19065–19076.
- D'ANGELO, N. & SONG, B. 1990 The Kelvin–Helmholtz instability in dusty plasmas. *Planet. Space Sci.* **38** (12), 1577–1579.
- DE ANGELIS, U., FORMISANO, V. & GIORDANO, M. 1988 Ion plasma waves in dusty plasmas: Halley's comet. *J. Plasma Phys.* **40** (03), 399–406.
- DU, C.R., NOSENKO, V., THOMAS, H.M., LIN, Y.F., MORFILL, G.E. & IVLEV, A.V. 2019 Slow dynamics in a quasi-two-dimensional binary complex plasma. *Phys. Rev. Lett.* **123** (18), 185002.
- DU, C.R., SÜTTERLIN, K.R., JIANG, K., RÄTH, C., IVLEV, A.V., KHRAPAK, S., SCHWABE, M., THOMAS, H.M., FORTOV, V.E., LIPAEV, A.M., *et al.* 2012 Experimental investigation on lane formation in complex plasmas under microgravity conditions. *New J. Phys.* **14** (7), 073058.
- DUAN, W.S. 2001 Weakly two-dimensional dust acoustic waves. *Phys. Plasmas* **8** (8), 3583–3586.
- DUAN, W.S. & PARKES, J. 2003 Dust size distribution for dust acoustic waves in a magnetized dusty plasma. *Phys. Rev. E* **68** (6), 067402.
- DUAN, W.S. & SHI, Y.R. 2003 The effect of dust size distribution for two ion temperature dusty plasmas. *Chaos, Solitons Fractals* **18** (2), 321–328.
- DUAN, W.S., WAN, G.X., WANG, X.Y. & LIN, M.M. 2004 Waves in two-dimensional hexagonal crystal. *Phys. Plasmas* **11** (9), 4408–4413.
- DUAN, W.S., YANG, H.J., SHI, Y.R. & LÜ, K.P. 2007 The effects of Gaussian size distribution dust particles in a complex plasma. *Phys. Lett. A* **361**, 368–372.
- GHOSH, S., GUPTA, M.R., CHAKRABARTI, N. & CHAUDHURI, M. 2011 Nonlinear wave propagation in a strongly coupled collisional dusty plasma. *Phys. Rev. E* **83** (6), 066406.
- HARTMANN, P., DONKÓ, Z., KALMAN, G.J., KYRKOS, S., GOLDEN, K.I. & ROSENBERG, M. 2009 Collective dynamics of complex plasma bilayers. *Phys. Rev. Lett.* **103** (24), 245002.
- HONG, X.R., SUN, W., SCHWABE, M., DU, C.R. & DUAN, W.S. 2021 Reflection and transmission of an incident solitary wave at an interface of a binary complex plasma in a microgravity condition. *Phys. Rev. E* **104** (2), 025206.
- HORANYI, M. 1996 Charged dust dynamics in the solar system. *Annu. Rev. Astron. Astrophys.* **34** (1), 383–418.
- HORANYI, M. & GOERTZ, C.K. 1990 Coagulation of dust particles in a plasma. *Astrophys. J.* **361** (1), 155–161.
- HUSSAIN, S. & HASNAIN, H. 2017 Magnetosonic wave in pair-ion electron collisional plasmas. *Phys. Plasmas* **24** (3), 032106.
- ICHIMARU, S., IYETOMI, H. & TANAKA, S. 1987 Statistical physics of dense plasmas: thermodynamics, transport coefficients and dynamic correlations. *Phys. Rep.* **149** (2 and 3), 91–205.

- IVLEV, A.V., ZHDANOV, S.K., THOMAS, H.M. & MORFILL, G.E. 2009 Fluid phase separation in binary complex plasmas. *Europhys. Lett.* **85** (4), 45001.
- JAISWAL, S., BANDYOPADHYAY, P. & SEN, A. 2014 Theoretical study of head-on collision of dust acoustic solitary waves in a strongly coupled complex plasma. *Phys. Plasmas* **21** (5), 053701.
- JAISWAL, S., PUSTYLNİK, M.Y., ZHDANOV, S., THOMAS, H.M., LIPAЕV, A.M., USACHEV, A.D., MOLOTKOV, V.I., FORTOV, V.E., THOMA, M.H. & NOVITSKII, O.V. 2018 Dust density waves in a dc flowing complex plasma with discharge polarity reversal. *Phys. Plasmas* **25** (8), 083705.
- JIANG, K., HOU, L.J., IVLEV, A.V., LI, Y.F., DU, C.R., THOMAS, H.M., MORFILL, G.E. & SÜTTERLIN, K.R. 2011 Initial stages in phase separation of binary complex plasmas: numerical experiments. *Europhys. Lett.* **93** (5), 55001.
- KAW, P.K. & SEN, A. 1998 Low frequency modes in strongly coupled dusty plasmas. *Phys. Plasmas* **5** (10), 3552–3559.
- KILLER, C., BOCKWOLDT, T., SCHÜTT, S., HIMPEL, M., MELZER, A. & PIEL, A. 2016 Phase separation of binary charged particle systems with small size disparities using a dusty plasma. *Phys. Rev. Lett.* **116** (11), 115002.
- LIN, W., MURILLO, M.S. & FENG, Y. 2020 Universal relationship of compression shocks in two-dimensional yukawa systems. *Phys. Rev. E* **101** (1), 013203.
- MARCIANTE, M. & MURILLO, M.S. 2017 Thermodynamic and kinetic properties of shocks in two-dimensional yukawa systems. *Phys. Rev. Lett.* **118** (2), 025001.
- MELZER, A., NUNOMURA, S., SAMSONOV, D., MA, Z.W. & GOREE, J. 2000 Laser-excited mach cones in a dusty plasma crystal. *Phys. Rev. E* **62** (3), 4162–4176.
- MENDIS, D.A. & ROSENBERG, M. 1994 Cosmic dusty plasma. *Annu. Rev. Astron. Astrophys.* **32** (1), 419–463.
- MENZEL, K.O., ARP, O. & PIEL, A. 2010 Spatial frequency clustering in nonlinear dust-density waves. *Phys. Rev. Lett.* **104** (23), 235002.
- MEURIS, P., VERHEEST, F. & LAKHINA, G.S. 1997 Influence of dust mass distributions on generalized Jeans–Buneman instabilities in dusty plasmas. *Planet. Space Sci.* **45** (4), 449–454.
- MORFILL, G.E. & THOMAS, H.M. 1996 Plasma crystal. *J. Vac. Sci. Technol.* **14** (2), 490–495.
- NUNOMURA, S., GOREE, J., HU, S., WANG, X. & BHATTACHARJEE, A. 2002 Dispersion relations of longitudinal and transverse waves in two-dimensional screened Coulomb crystals. *Phys. Rev. E* **65** (6), 066402.
- RAO, N.N., SHUKLA, P.K. & YU, M.Y. 1990 Dust-acoustic waves in dusty plasmas. *Planet. Space Sci.* **38** (4), 543–546.
- ROTHERMEL, H., HAGL, T., MORFILL, G.E., THOMA, M.H. & THOMAS, H.M. 2002 Gravity compensation in complex plasmas by application of a temperature gradient. *Phys. Rev. Lett.* **89** (17), 175001.
- SCHWABE, M., KHRAPAK, S.A., ZHDANOV, S.K., PUSTYLNİK, M.Y., RÄTH, C., FINK, M., KRETSCHMER, M., LIPAЕV, A.M., MOLOTKOV, V.I., SCHMITZ, A.S., *et al.* 2020 Slowing of acoustic waves in electrorheological and string-fluid complex plasmas. *New J. Phys.* **22** (8), 083079.
- SCHWABE, M., ZHDANOV, S.K., THOMAS, H.M., IVLEV, A.V., RUBIN-ZUZIC, M., MORFILL, G.E., MOLOTKOV, V.I., LIPAЕV, A.M., FORTOV, V.E. & REITER, T. 2008 Nonlinear waves externally excited in a complex plasma under microgravity conditions. *New J. Phys.* **10** (3), 033037.
- SHUKLA, P.K. & ELIASSON, B. 2012 Nonlinear dynamics of large-amplitude dust acoustic shocks and solitary pulses in dusty plasmas. *Phys. Rev. E* **86** (4), 046402.
- SHUKLA, P.K. & SILIN, V.P. 1992 Dust ion-acoustic wave. *Phys. Scr.* **45** (5), 508.
- SMITH, B., HYDE, T., MATTHEWS, L., REAY, J., COOK, M. & SCHMOKE, J. 2008 Phase transitions in a dusty plasma with two distinct particle sizes. *Adv. Space Res.* **41** (9), 1510–1513.
- SUN, W., SCHWABE, M., THOMAS, H.M., LIPAЕV, A.M., MOLOTKOV, V.I., FORTOV, V.E., FENG, Y., LIN, Y.F., ZHANG, J., GUO, Y., *et al.* 2018 Dissipative solitary wave at the interface of a binary complex plasma. *Europhys. Lett.* **122** (5), 55001.
- TAO, L.L., WANG, F.P., GAO, D.N., ZHANG, H. & DUAN, W.S. 2020 Effect of the pressure of the dust grains in strongly coupled dusty plasma on the head-on collision between two nonlinear waves. *J. Plasma Phys.* **86** (1), 1–11.

- TSAI, Y.Y., TSAI, J.Y. & I, L. 2016 Generation of Acoustic Rogue Waves in Dusty Plasmas Through Three-dimensional particle focusing by distorted waveforms. *Nat. Phys.* **12** (6), 573–577.
- WANG, X., BHATTACHARJEE, A. & HU, S. 2001 Longitudinal and transverse waves in yukawa crystals. *Phys. Rev. Lett.* **86** (12), 2569.
- WANG, X., SCHWAN, J., HSU, H.W., GRÜN, E. & HORÁNYI, M. 2016 Dust charging and transport on airless planetary bodies. *Geophys. Res. Lett.* **43** (12), 6103–6110.
- WIEBEN, F., SCHABLINSKI, J. & BLOCK, D. 2017 Generation of two-dimensional binary mixtures in complex plasmas. *Phys. Plasmas* **24** (3), 033707.
- WYSOCKI, A., RÄTH, C., IVLEV, A.V., SÜTTERLIN, K.R., THOMAS, H.M., KHRAPAK, S., ZHDANOV, S., FORTOV, V.E., LIPAEV, A.M. & MOLOTKOV, V.I. E. A. 2010 Kinetics of fluid demixing in complex plasmas: role of two-scale interactions. *Phys. Rev. Lett.* **105** (4), 045001.
- YANG, L., SCHWABE, M., ZHDANOV, S., THOMAS, H.M., LIPAEV, A.M., MOLOTKOV, V.I., FORTOV, V.E., ZHANG, J. & DU, C.R. 2017 Density waves at the interface of a binary complex plasma. *Europhys. Lett.* **117** (2), 25001.
- ZHANG, H., WANG, X.Y., DUAN, W.S. & YANG, L. 2016 Effects dust size distribution on transportation of dust grains in a weakly ionized plasma. *Indian J. Phys.* **90** (10), 1207–1213.
- ZHANG, H., YANG, Y., HONG, X.R., QI, X., DUAN, W.S. & YANG, L. 2017 Freak oscillation in a dusty plasma. *Phys. Rev. E* **95** (5), 053207.